Long Term Process-Based Morphological Modelling of Pocket Beaches

A case study in Singapore using XBeach

C.W.T. (Cas) Van Bemmelen

4219163

Additional Thesis (CIE5050-09)
Hydraulic Engineering and Water Resources Management (HEWRM)

Technical University Delft
Faculty of Civil Engineering and Geosciences

and

National University of Singapore
Department of Civil & Environmental Engineering

April 4, 2017

Supervision by:

Prof. dr. ir. S.G.J. (Stefan) Aarninkhof	Delft University of Technology
Dr. ir. M.A. (Matthieu) De Schipper	Delft University of Technology
Ir. M.H.P. (Maarten) Jansen	Witteveen + Bos
Ir. W.P. (Willem) Bodde	Witteveen + Bos

Outline of this Study

Pocket beaches comprise a large part of the world's coastline and their behaviour is of great interest to coastal scientists and engineers. This study assesses the morphological response of these systems under (oblique and normal) wave attack and is split up into two parts; an analysis of schematized model setups and a case study. Prior to these two parts, a general introduction into the subject of pocket beaches is given.

In the first part, schematized model setups are used to validate the applicability of XBeach. Due to the lack of measurements to compare the obtained model results, qualitative checks have been derived based on the expected hydrodynamics and morphological changes within pocket beaches. This is followed by a description of the model, initial bathymetry and the applied wave conditions. Finally, the model settings, the results, discussion and conclusion of this part are presented.

In the second part, a model setup is made for Tanjong Beach in Singapore. This part starts with an overview of the study area, followed by a description of the (assumed) environmental conditions. Next, the model setup and skill assessment are treated. Finally, the results, discussion and conclusion of this part are presented.

Four appendices are attached that support the main document, followed by an overview of the used literature during this study.

Long Term Process-Based Morphological Modelling of Pocket Beaches

A case study in Singapore using XBeach

C.W.T. Van Bemmelen

Delft University of Technology, Faculty of Civil Engineering and Geosciences, The Netherlands
National University of Singapore, Department of Civil Engineering, Singapore

Abstract: The applicability of the open source model XBeach was tested for pocket beaches in this paper. First, schematized model setups have been used to assess the performance of XBeach qualitatively. It was found that adjustments of the initial bed were required to obtain the expected hydrodynamic conditions. The default sediment advection calibration factors had to be increased to obtain the expected morphological response of the pockets (stationair: 0.15, surfbeat: 0.30). The results have shown that the surfbeat mode outperforms the stationary mode based on a qualitative assessment. It was furthermore found that wave-current interaction produced unreliable results and should be avoided when modelling pocket beaches using XBeach. Non-hydrostatic simulations produced significantly more sedimentation behind the headlands due to the inclusion of diffraction. This mode was found to produce unexpected erosion at the upper shoreface however, indicating the inapplicability of the sediment transport formulas in non-hydrostatic simulations. Expansion of the classic pocket beach into two adjacent pocket beaches showed that these systems have to be treated as a complete system if interactions between these pockets are expected (separated by a salient). It was found that an individual assessment is adequate if a tombolo separates the pockets. Second, the morphological developments between the year 2000 and 2015 at Tanjong Beach (Singapore) were modelled using XBeach. For the modelled bed level changes, which were compared to bathymetric measurements, a 'Good' Mean-Squared Error Skill Score of 0.31 was found. In the prepared model, the obtained sediment advection calibration factors from the first part were used and model calibration was not performed. Based on the schematizations and the case study performed in this study, XBeach was found to be applicable for long term process-based modelling of pocket beaches.

Keywords: Pocket Beaches, Embayed Beaches, Nearshore Currents, Morphology, XBeach

---

Introduction

More than half of the world's coastline (51%) is characterized by headland-bay morphological features (Short and Masselink, 1999). These coastline types are often referred to as pocket beaches or embayed beaches. Generally, pocket beaches can be described as beaches that are contained between two (hardrock) headlands. Wave energy tends to focus on these headlands, causing headland erosion, and disperse in the bay, causing bay filling.

From the beginning of the 20th century, geologists and geographers have shown great interest in the coastal response to wave conditions. Halligan (1906) and Lewis (1938) were the first to recognize the phenomenon of bay shape orientation. In order to cater to the demands of Coastal Zone Management after the 1960s, various methods have been developed by coastal engineers to predict shoreline behaviour. For example, Silvester (1960) was the first to promote the concept of a stable bay beach. Various empirical models were based on this concept, with the most successful being the Parabolic Bay Shape Equation (PBSE) developed by Hsu and Evans (1989). This equation has proven to be valuable in the engineering community and is used by many coastal scientists around the world. (Hsu et al., 2010)

Aside from this empirical method, a statistical method called the Principal Component Analysis (also known as Empirical Orthogonal Function (EOF)) is often used to decompose coastal datasets into spatial and temporal patterns (Dail et al., 2000; Harley et al., 2011). These patterns, known as eigenfunctions, can be related to various beach processes (Aubrey, 1979). Further research by Harley et al. (2015) using EOF shows that beach rotation within embayed beaches is highly depended on the alongshore variability in cross-shore processes. For site specific cases it has been shown that the EOF method is capable of explaining various coastal processes (Harley et al., 2011; Turki et al., 2013). It is still unknown whether this holds for all embayed beaches in general.

The empirical PBSE is limited by the fact that wave conditions and nearshore processes cannot be taken into account. It is therefore impossible to play 'what-if' games using these type of empirical formulations. The statistical EOF method requires large amounts of high quality site specific data and is often not suitable for predicting coastal response to human interventions. As a result, the performance of engineering solutions to coastal issues cannot be assessed using these methods. With the advances in numerical coastal models and increasing computing power, process based modelling could be of great use in predicting the behaviour of pocket beaches.

Numerical process-based modelling by Daly et al. (2011) showed that it is indeed possible to simulate long term morphological responses of pocket beaches forced by various wave conditions. Their study showed (using Delft3D) that the shoreline rotation is mainly dependent on the incident wave direction and the directional spreading. In addition to shoreline rotation, a study performed by Ratliff and Murray (2014) showed that a newly found breathing mode can also be identified. This breathing mode is best described as the changes of shoreline curvature within embayed beaches. A further understanding of the hydrodynamic conditions within pocket beaches is presented in Castelle and Coco (2013). This study is in line with findings of Reniers et al. (2007) and has indicated the impact of Very Low Frequency motions (VLFs) on floating material and headland rips on surfzone flushing.

Gap of Knowledge and Objectives

This research focusses on the applicability of XBeach in case studies on long term morphology of pocket beaches. Delft3D has been used in the past to study the long term morphodynamic behaviour of pocket beaches (Daly et al., 2011). It is unknown however, whether XBeach is applicable in studies concerning these long term pocket beach developments.

The main objective of this research is to determine whether XBeach is suitable for modelling long term morphological changes in pocket beaches. A model setup is prepared, in which schematized pocket beaches are used to assess the performance of XBeach qualitatively.

The secondary objective is to prepare a long term morphological model based on the findings of these schematized pocket beach studies. This XBeach model is made for Tanjong Beach at Sentosa (Singapore) and is carried out for Witteveen+Bos (W+B). The model setup and parameter settings are partly based on the results of the first part. In this part, the XBeach model results are compared (quantitatively) to bathymetric measurements.

Part I
Pocket Beach Schematizations

Schematized model setups have been used to assess whether XBeach is capable of reproducing the processes within pocket beaches. First, an overview of the governing hydrodynamic and morphological processes is given. This first analysis results in a list of processes that have to be represented within the model. Second, schematized model setups are constructed based on the study by Daly et al. (2011). Results obtained from these models are then compared (qualitatively) to the list of expected processes.

EXPECTED HYDRODYNAMICS AND MORPHOLOGY

Compared to open beaches, pocket beaches show a different response to wave forcing due to their headlands. It is therefore important to describe the expected hydrodynamic conditions and morphological response beforehand. This section describes the processes that are expected to occur within a pocket beach. The first overview of processes is done with 'shore normal' waves (270 degrees nautical). In the second overview, the pocket beaches are under oblique wave attack (i.e. 250 degrees nautical). A series of qualitative checks (*QC x.y*) have been derived for these cases, supported by a visual representation of the processes (see Figure 1).

Normally Incident Waves (270°)

QC 1.1 The waves approaching the pocket beach will shoal in front of the headlands, increasing the shoreward directed wave force. This force will be compensated by a local water level decrease, the wave set-down. In the breaker zone, a shoreward directed force will be generated by the breaking waves. This force will be compensated by a local water level increase, the wave set-up. These water level variations in front of the headlands will not occur at the pocket beach entrance, causing a net inflow to occur around the headlands.

QC 1.2 Inside the pocket longshore currents and water level setup differences govern the flow patterns. The longshore currents will be generated due to the orientation of the shoreline with respect to the incoming waves. Where these longshore currents meet, a rip current is expected. At the transition zone from exposed to sheltered coastline however, the water level setup differences cause a flow (parallel to the coastline) towards the 'corners' of the pocket beach.

QC 1.3 Behind the headlands, vortices will be generated due to a gradient in radiation stresses caused by wave sheltering. These currents increase the sediment transported towards the 'corners' of the pocket.

QC 1.4 Erosion will occur at the transition between the exposed and sheltered shoreline. Sedimentation will occur in the 'corners' and centre of the pocket. The exposed shoreline will therefore straighten and become perpendicular to the wave direction.

QC 1.5 Straightening of the coastline will have a positive feedback on the formation of the rip current, which will decay.

QC 1.6 Sedimentation behind the headlands is expected, due to the reduced wave-induced sediment stirring and the longshore transport towards these sheltered areas.

Oblique Waves (250°)

QC 2.1 Waves approaching the pocket will cause a longshore current along the headlands, causing inflow from the up-drift headland and outflow from the down-drift headland.

QC 2.2 Inside the pocket, a longshore current will be generated due to the orientation of the shoreline with respect to the incoming waves. This current feeds the outflow from the down-drift headland.

QC 2.3 Sedimentation will occur behind the down-drift headland due to the direction of sediment transport generated by the longshore current inside the pocket. Erosion will mainly occur behind the up-drift headland, caused by a lack of sediment supply to feed the longshore transport.

QC 2.4 These sedimentation and erosion patterns will cause the shoreline to rotate, orienting itself perpendicular to the incident wave angle.

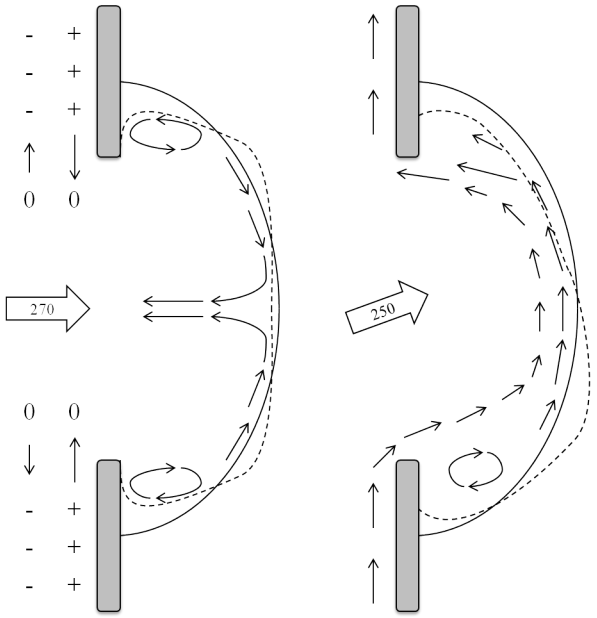

Figure 1: Flow patterns (arrows) inside the pocket beaches prior to morphological development (solid line). Water level set-up zones are indicated with '+', water level set-down zones with '-' and zero set-up with '0'. The coastline response of this system to the given wave direction is given by the dashed line.

MODEL SETUP

Model Description

In this study the Kingsday Release (Version 1.22) of the open source model XBeach (Roelvink et al., 2009) is used. This numerical model has been developed to study hydrodynamic and morphodynamic processes within coastal areas by solving coupled 2DH equations. For the hydrodynamic processes, the model includes short wave transformation (refraction, shoaling and breaking), long wave transformation (generation, propagation and dissipation) and flow (Roelvink et al., 2015). Morphodynamic processes are mostly represented by bed load and suspended sediment transport combined with bed updating and avalanching of the dune face. Three hydrodynamic modes are available within XBeach;

1. Stationary wave mode (short wave averaged, hydrostatic)
2. Surfbeat mode (instationary, short wave averaged, hydrostatic)
3. Non-hydrostatic mode (wave-resolving)

All modes will be used in this study, to assess the importance of the included processes in each mode. Although computationally expensive (due to the high spatial resolution that is required), wave-resolved modelling is needed to assess the importance of diffraction around the headlands. This hydrodynamic process is not included in the short wave averaged modes.

Model Formulation

In sum, the XBeach model solves the Shallow Water Equations (SWEs) for long waves and a wave action balance equation for short waves. For the long waves a Generalised Lagrangian Mean (GLM) approach is applied,

$$\frac{\partial u^L}{\partial t} + u^L\frac{\partial u^L}{\partial x} + v^L\frac{\partial u^L}{\partial y} - fv^L - \nu_h\left(\frac{\partial^2 u^L}{\partial x^2} + \frac{\partial^2 u^L}{\partial y^2}\right) = \frac{\tau_{sx}}{\rho h} - \frac{\tau^E_{bx}}{\rho h} - g\frac{\partial \eta}{\partial x} + \frac{F_x}{\rho h} - \frac{F_{v,x}}{\rho h} \quad (1)$$

$$\frac{\partial v^L}{\partial t} + u^L\frac{\partial v^L}{\partial x} + v^L\frac{\partial v^L}{\partial y} - fu^L - \nu_h\left(\frac{\partial^2 v^L}{\partial x^2} + \frac{\partial^2 v^L}{\partial y^2}\right) = \frac{\tau_{sy}}{\rho h} - \frac{\tau^E_{by}}{\rho h} - g\frac{\partial \eta}{\partial y} + \frac{F_y}{\rho h} - \frac{F_{v,y}}{\rho h} \quad (2)$$

$$\frac{\partial \eta}{\partial t} + \frac{\partial hu^L}{\partial x} + \frac{hv^L}{\partial y} = 0 \quad (3)$$

Where u^L and v^L are the Langrangian velocities, f is the Coriolis coefficient, ν_h is the horizontal viscosity, τ_{sx} and τ_{sy} are the wind shear stresses, F_x and F_y are the wave induced stresses and $F_{v,x}$ and $F_{v,y}$ are the stresses induced by vegetation. Non-hydrostatic XBeach calculations are done with a dynamic pressure correction, making a separate description of the short waves unnecessary. Stationary and surfbeat calculations do however rely on the wave-action balance equation (see Eq. 5).

The wave induced stresses, which are a source term in these shallow water equations, are formed from two balance equations: the wave-action and roller energy balance equations. Wave action (A) is defined as follows,

$$A(x, y, z, \theta) = \frac{S_W(x, y, t, \theta)}{\sigma(x, y, t)} \quad (4)$$

Where S_W and σ are the directional bin and intrinsic wave frequency respectively. The wave-action balance equation is defined as follows,

$$\frac{\partial A}{\partial t} + \frac{\partial c_{gx}A}{\partial x} + \frac{\partial c_{gy}A}{\partial y} + \frac{\partial c_{g\theta}A}{\partial \theta} = -\frac{D_W + D_f + D_v}{\sigma} \quad (5)$$

Where c_g is the propagation velocity of the wave action (group velocity) and D_W is the wave energy dissipation term. This energy dissipation is a source term in the roller energy balance equation,

$$\frac{\partial E_r}{\partial t} + \frac{\partial E_r c\cos\theta}{\partial x} + \frac{\partial E_r c\sin\theta}{\partial y} = D_W - D_r \quad (6)$$

Where E_r is the roller energy (per bin) and D_r is the roller energy dissipation term. At the core of the sediment transport module in XBeach[1], a depth-averaged advection-diffusion scheme (Galappatti and Vreugdenhil, 1985) including the effects of wave skewness and asymmetry is used,

$$\frac{\partial hC}{\partial t} + \frac{\partial hC(u^E - u_a\sin\theta)}{\partial x} + \frac{\partial hC(v^E - u_a\cos\theta)}{\partial y} + \frac{\partial}{\partial x}\left[D_h h\frac{\partial C}{\partial x}\right] + \frac{\partial}{\partial y}\left[D_h h\frac{\partial C}{\partial y}\right] = \frac{hC_{eq} - hC}{T_s} \quad (7)$$

Where C is the sediment concentration, C_{eq} is the equilibrium sediment concentration, D_h is the sediment diffusion coefficient and T_s is the adaptation time (speed of the sediment response). The right hand side of this equation can be seen as the erosion (hC_{eq}) and deposition (hC) terms. It can furthermore be observed that Eq. 7 makes use of the Eulerian velocities (u^E, v^E) whereas the SWEs use the Lagrangian velocities (u^L, v^L). The difference between these velocities lies within the inclusion of the Stokes drift ($u^L = u^E + u^S$, $v^L = v^E + v^S$).

[1] It is important to note that this module has not been developed and validated for the non-hydrostatic mode. It is however used to assess the importance of diffraction in this study.

Two formulations are available within XBeach for the equilibrium sediment concentration; Soulsby-Van Rijn and Van Thiel-Van Rijn (default). In both of these formulations, the total equilibrium sediment concentration is based on a combination of bed and suspended equilibrium concentrations ($C_{eq,b}$, $C_{eq,s}$). It has been shown that Van Thiel-Van Rijn ($C_{eq,b} \sim U^{1.5}$, $C_{eq,s} \sim U^{2.4}$) is preferred over Soulsby-Van Rijn ($C_{eq,b} \sim U^{2.4}$, $C_{eq,s} \sim U^{2.4}$) in models including overwash and breaching (De Vet, 2014). It is still unknown whether this also holds for pocket beaches.

The effect of wave shape on the sediment advection velocity u_a is calculated using a discretized formulation (van Thiel de Vries, 2009),

$$u_a = (f_{Sk} S_k - f_{As} A_s) u_{rms} \tag{8}$$

In this equation, the root-mean-squared velocity (u_{rms}) is multiplied by a combination of wave skewness (S_k), wave asymmetry (A_s) and two calibration factors (f_{Sk}, f_{As}). Larger values for these calibration factors result in higher values for u_a, which in turn causes a stronger onshore sediment transport. This equation is not used for the non-hydrostatic simulations due to the fact that the asymmetry and skewness are directly computed in this hydrodynamic mode. Bed level changes are determined using the sediment mass conservation equation,

$$\frac{\partial z_b}{\partial t} + \frac{f_{mor}}{1-p}\left(\frac{\partial q_x}{\partial x} + \frac{\partial q_y}{\partial y}\right) = 0 \tag{9}$$

Where the porosity is represented by p, q_x and q_y are sediment rates in horizontal directions and z_b is the bed level. The morphological acceleration factor (f_{mor}) speeds up the morphological development by exaggerating the sediment fluxes within the model. Reference is made to the manual for a more detailed overview of the equations, boundary conditions and numerical implementation in XBeach (Roelvink et al., 2015).

Model Extent and Initial Bathymetry

The model extent was based on the setup presented in Daly et al. (2011), which used Delft3D to assess pocket beach morphology. The dimensions of the headlands, gap and extent of the model were kept the same. The width of the gap is equal to 1200 m and the length of each headland is equal to 600 m. Empirical equilibrium formulations were used to obtain the initial bathymetry based on the dimensions presented.

First, the PBSE as presented in Hsu and Evans (1989) was used to find the equilibrium shoreline. This equation holds as follows,

$$\frac{R}{R_0} = C_0 + C_1\left(\frac{\beta}{\theta}\right) + C_2\left(\frac{\beta}{\theta}\right)^2 \tag{10}$$

Where the main parameters are β, the angle formed between wave crest and the control line, and R_0, the length of the control line. The parameter θ represents the angle between the wave crest line and the coastline. The coefficients C_0, C_1 and C_2 depend on the value of β (which were obtained from Table 2 in Hsu and Evans (1989)). The control lines had their origin at either tip of the headland and intersect the coastline at an angle of 37°.

Second, the Dean profile was used to obtain the equilibrium cross-shore bathymetry. This profile can be obtained using the following equation,

$$h(y) = A * y^{2/3} \tag{11}$$

Where h is the water depth, y is the distance to the shoreline and A represents the sediment dependent scale parameter. By choosing a median grain diameter (D_{50}) of 0.3 mm, the value for A equals 0.13 $m^{1/3}$ (obtained from Figure 1 in Dean (1991)). The resulting pocket beach bathymetry can be seen in Figure 2.

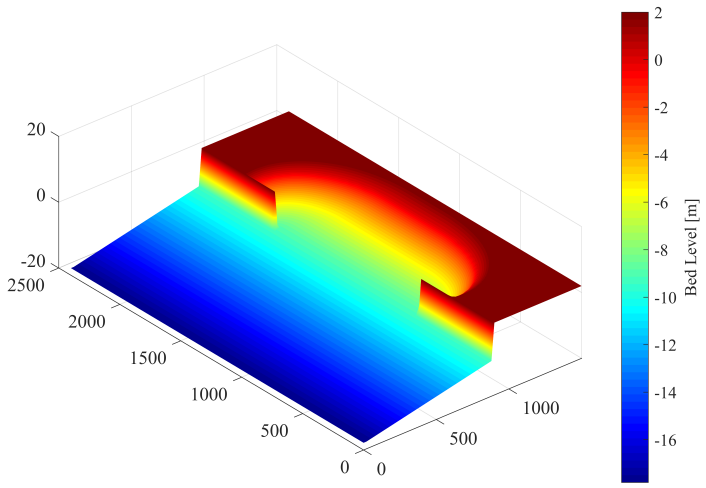

Figure 2: The initial bathymetry used in Part 1 of this study.

Wave Conditions

Forcing of the model was based on the wave conditions presented in Daly et al. (2011), which used the SWAN wave module in Delft3D. Their paper showed the relative importance of these parameters on the morphological development of pocket beaches. Two combinations of wave characteristics were selected, with a varying main wave direction (Dir). XBeach was forced with a JONSWAP spectrum for the wave boundary conditions. This spectrum requires H_{m0} (estimate of the significant wave height), T_p (the peak wave period), Dir (the main wave angle), Gammajsp (the peak enhancement factor) and Dspr (the directional spreading). Table 1 provides an overview of the wave parameters used in this study. The peak enhancement factor, which is used in SWAN corresponds to the factor used in XBeach (both default 3.3). Note that it was assumed however that the directional spreading, which is defined using a cosine power M relation in SWAN equals 2*s in the cosine power relation of XBeach.

Parameter	Value(s)	
H_{m0}	2	m
T_p	12.0	s
Dir	250/270	deg
Gammajsp	3.3	[-]
Dspr(s)	10	[-]

Table 1: Wave parameters (JONSWAP) used in Part 1.

Model Settings

The three hydrodynamic modes (2D) within XBeach include different processes and require different settings and parameter selections. Initially, these modes were used in combination with the default XBeach settings (see Appendix D obtained from Roelvink et al. (2015)). These default values were used throughout this study, if not specified otherwise. Hydrostatic XBeach simulations were done using a Cartesian grid (as used in Daly et al. (2011)) with dx = 20 m and dy = 20 m. For these simulations, a morphological acceleration factor of 10 was used to increase the bed level changes which reduced overall computation time (see Eq. 9). Non-hydrostatic simulations were done using a Cartesian grid with dx = dy = 4 m and a morphological acceleration factor of 50 to keep computational times acceptable. Due to the symmetrical model setup, cyclic boundary conditions were very suitable and were therefore applied to all model calculations. These boundary conditions increase computational efficiency by copying the conditions (waves, flow and sediment transport) to each other.

For stationary simulations, the Baldock wave breaking formulation was used (Baldock et al., 1998). It was recommended by Deltares (personal communication with R. McCall) that the breaker parameter (γ) had to be increased to 0.78 with respect to the default value (0.55) when using the Baldock formulation. This formulation makes use of the breaker height to compute the wave energy dissipation (D_W),

$$H_b = \frac{0.88}{k} \tanh\left[\frac{\gamma k h}{0.88}\right] \tag{12}$$

Where k is the wave number and h is the water depth. In this formulation, wave breaking is governed by the wave steepness for deep water conditions ($kh \rightarrow \infty$) and depth-induced wave breaking occurs for shallow water conditions ($kh \rightarrow 0$). By increasing the breaker parameter, larger waves are allowed to approach the shoreline, resulting in a higher wave impact.

Surfbeat simulations were done with the Roelvink1 formulation, in which the default XBeach values are applied. In essence, this formulation gives an estimate for the amount of dissipation per wave breaking event. The breaker parameter (γ) can be found in the determination of the maximum wave height (H_{max}), which is based on a combination of water depth (h) and a fraction of the wave height (H_{rms}).

$$H_{max} = \gamma(h + \delta H_{rms}) \tag{13}$$

Non-hydrostatic simulations did not require a separate breaker formulation, this mode within XBeach makes use of the bore like behaviour of breaking waves (Smit et al., 2010).

Interaction between the mean flow and waves have shown to be important when dealing with rip-currents (Reniers et al., 2007). It has even been shown that neglecting wave-current interaction can result in instabilities of rip currents (Yu and Slinn, 2003). In order to assess the impact of this interaction within XBeach, simulations were performed with and without wave-current interaction (WCI). Wave-current interaction is represented in XBeach by correcting the wave number using the Eikonal equations. This correction has an impact on the group and wave propagation speed (see bold terms that have to be added due to WCI),

$$c_x(x, y, t, \theta) = c_g \cos\theta + \boldsymbol{u^L} \tag{14}$$

$$c_y(x, y, t, \theta) = c_g \cos\theta + \boldsymbol{v^L} \tag{15}$$

$$\begin{aligned} c_\theta(x, y, t, \theta) = {} & \frac{\sigma}{\sinh 2kh}\left(\frac{\partial h}{\partial x}\sin\theta - \frac{\partial h}{\partial y}\cos\theta\right) \\ & + \cos\boldsymbol{\theta}\left(\sin\boldsymbol{\theta}\frac{\boldsymbol{\partial u}}{\boldsymbol{\partial x}} - \cos\boldsymbol{\theta}\frac{\boldsymbol{\partial u}}{\boldsymbol{\partial y}}\right) + \sin\boldsymbol{\theta}\left(\sin\boldsymbol{\theta}\frac{\boldsymbol{\partial v}}{\boldsymbol{\partial x}} - \cos\boldsymbol{\theta}\frac{\boldsymbol{\partial v}}{\boldsymbol{\partial y}}\right) \end{aligned} \tag{16}$$

As previously stated in the Model Formulation, two sediment transport formulations are available in this model. The default Van Thiel-Van Rijn formulation was used initially. The performance of this transport formulation was then compared to the performance of Soulsby-Van Rijn.

RESULTS

The results in this section have been described and compared to the qualitative checks presented on Page 3. First, the hydrodynamics and morphological changes are presented for the stationary wave model. Based on these results, adjustments to the model setup have been made according to the qualitative checks. Second, surfbeat and non-hydrostatic calculations are presented which include these set-up adjustments.

Shoreline Straightening

Results of the stationary wave model showed that not all hydrodynamic conditions were simulated as expected (see Figure 3a). With and without WCI, the predicted net inflow around the headlands was not present (*QC 1.1*). For both of these simulations, this was attributed to the lack of (depth induced) wave breaking in front of the headland calculated using Eq. 12. Therefore, the expected water level difference across the pocket entrance did not occur. Note that the exact opposite was modelled with WCI, an outflow occurred around the headlands. The initial hydrodynamic conditions within the pocket itself showed reasonable similarity to what one would expect from these systems (see Figure 3a, c). Both initial conditions showed a rip current in the centre of the pocket (*QC 1.2*). Current-induced wave refraction within the WCI simulation resulted in a more parallel longshore current. The rip current generated with WCI was more narrow, but a smaller (offshore directed) Eulerian velocity was generated. Vortices formed behind the headlands, caused by a difference in radiation stresses between the exposed and sheltered areas (*QC 1.3*). The morphological developments for both simulations were not as expected (Figure 3b, d). The models showed a retreat of the coastline instead of the expected straightening, in strong contrast to *QC 1.4*. The rip current did decay however and sedimentation behind the headlands was visible (*QC 1.5* and *QC 1.6*).

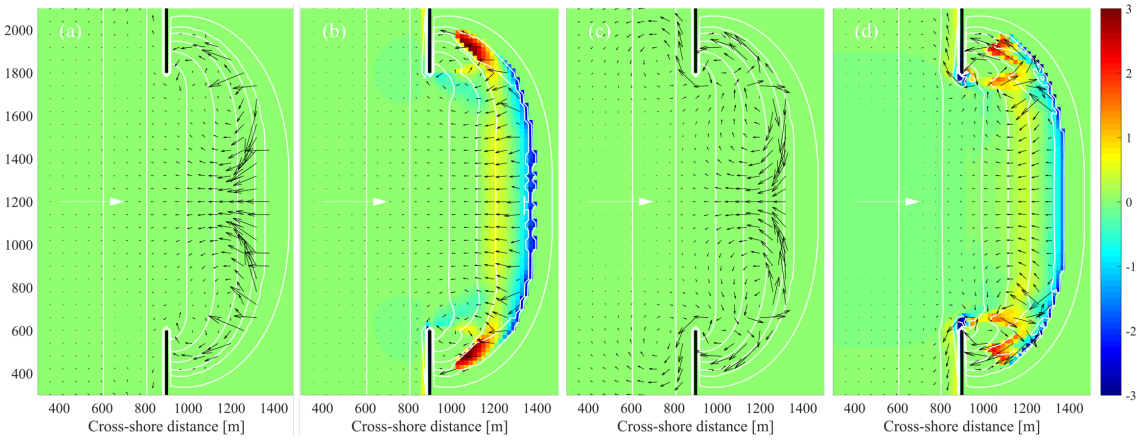

Figure 3: Initial conditions of the pocket beach hydrodynamics given for simulations without (a) and with (c) WCI enabled. Sedimentation and erosion results for simulations of 4 years are given in (b) and (d) respectively. Depth contour lines are given in white, ranging from -12 meters to +2 meters with intervals of 2 meters. Black vectors indicate the Eulerian velocity directions. The white arrow indicates the mean wave direction and its length corresponds to 1 m/s. The following wave climate was applied: H_s = 2 m, T_{m01} = 10 s, Dir = 270° and Dspr = 10.

Several methods were developed to achieve the expected hydrodynamic behaviour in front of the headlands. Amongst others, a linearly varying foreshore was introduced in front of the headlands. It was found that this solution can provide more reasonable flow patterns in front of the headland, but erosion of this slope caused unrealistic sedimentation within the pocket beach. The most effective method to achieve the expected flow conditions was found to be a rapid decrease of the water depth just in front of the headlands. Two cells (representing 40 meters) were given a water depth of 2 meters and were non-erodible. This caused the waves to break in front of the headlands, resulting in a better representation of the hydrodynamic conditions of a pocket beach. These variations in wave height induced the expected water level gradient, resulting in a net inflow around the headlands.

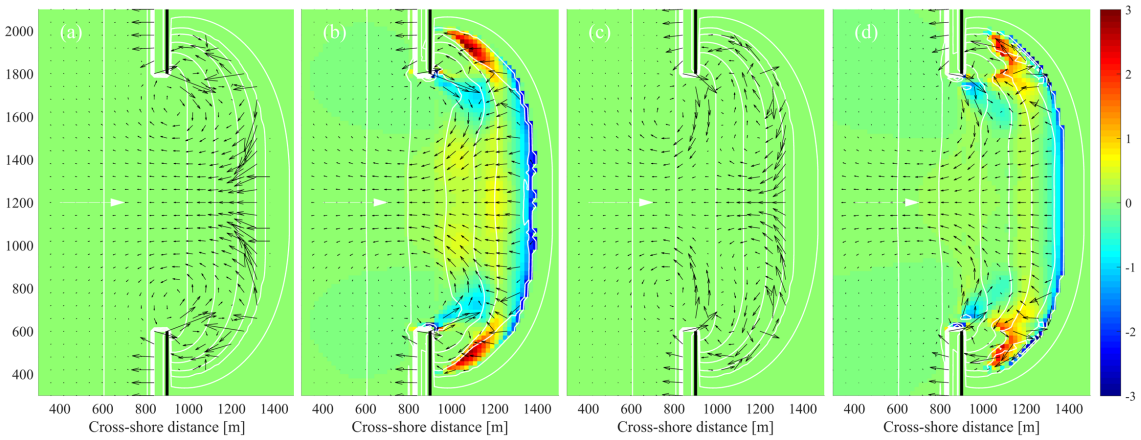

Figure 4: Hydrodynamic conditions and morphological response with the additional foreshore. Initial conditions are given for simulations without (a) and with (c) WCI enabled. Sedimentation and erosion results for simulations of 4 years are given in (b) and (d) respectively. Depth contour lines are given in white, ranging from -12 meters to +2 meters with intervals of 2 meters. Black vectors indicate the Eulerian velocity directions. The white arrow indicates the mean wave direction and its length corresponds to 1 m/s. The following wave climate was applied: H_s = 2 m, T_{m01} = 10 s, Dir = 270° and Dspr = 10.

Sediment Transport Formulation

The results presented in the previous sections were obtained using the (default) Van Thiel-Van Rijn formulation. Due to the fact that sedimentation behind the headlands was rather limited and the shoreline response was not as expected, the performance of Soulsby-Van Rijn became of great interest. As previously stated, it was expected that the latter formulation would produce more sediment transport. The default settings for the sediment formulations were used and WCI was enabled for this comparison.

Based on *QC 1.4*, in which it is assumed that the shoreline will straighten due to a combination of sedimentation in the pocket centre and erosion in transition zone, it can be seen that the Van Thiel-Van Rijn outperformed the Soulsby-Van Rijn formulation (see Figure 5). Sedimentation behind the headlands (*QC 1.6*) did occur in higher quantities when using the Soulsby-Van Rijn formulation, but this did not outweigh the increased erosion in the pocket centre. The Van Thiel-Van Rijn formulation was therefore used in the upcoming XBeach formulations.

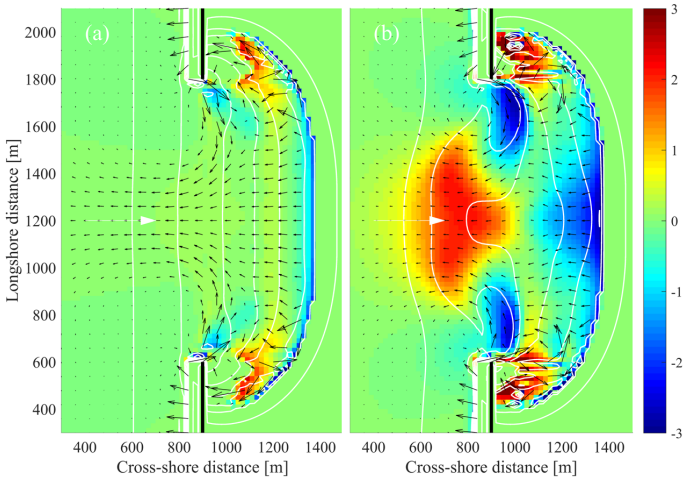

Figure 5: Comparison between the Van Thiel-Van Rijn (a) and Soulsby-Van Rijn (b) sediment transport formulas. Colours indicate sedimentation and erosion patterns after 4 years of morphological development. Wave current interactions are enabled and the black vectors indicate the Eulerian velocity directions. Depth contour lines are given in white, ranging from -12 meters to +2 meters with intervals of 2 meters. The white arrow indicates the mean wave direction and its length corresponds to 1 m/s. The following wave climate was applied: H_s = 2 m, T_{m01} = 10 s, Dir = 270° and Dspr = 10.

Wave Current Interaction

Results obtained from the simulations using Soulsby-Van Rijn showed a peculiar morphological response to the wave forcing. Behind the headlands 'lines' of deposited sediment could be observed. These strange sedimentation patterns only occurred when wave-current interaction was enabled. It turned out that the root-mean-squared wave height (based on the instantaneous wave energy) showed very similar patterns behind the headlands. Changing the parameters related to the WCI implementation in XBeach (*cats*, *hwci*) failed in reducing this effect behind the headlands. Parameters determining the method of model parallelization in XBeach (`MPI`) also had no impact on the WCI patterns. These unrealistic wave conditions behind the headlands could thus not be reduced and WCI was therefore not used in the upcoming model results presented in this study.

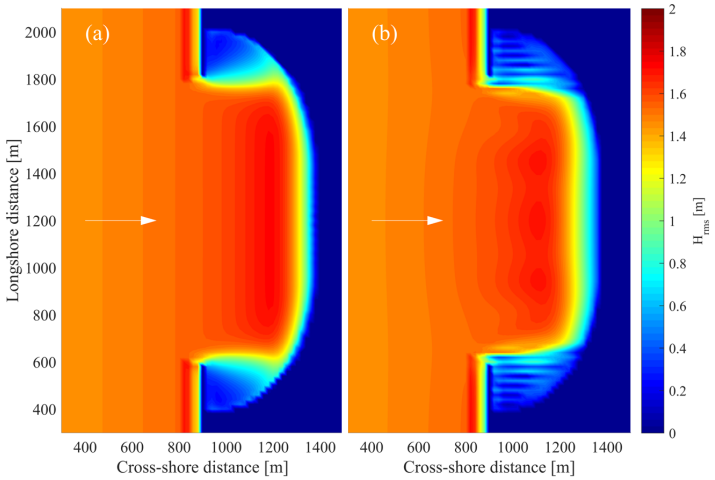

Figure 6: Comparison between computed wave heights H_{rms} without WCI (a) and with WCI (b).

Van Thiel-Van Rijn Calibration

After adjusting the headland bathymetry, XBeach still produced mixed results when the morphological response of the system was compared to the qualitative checks. The coastline response was not as expected when using the default sediment transport settings within XBeach.

QC 1.4 described sedimentation at the centre of the pocket and erosion in the corners of the pocket. Figure 4a depicts a retreat of the coastline in the centre of the bay. This retreat gradually reduced towards the headlands, which resulted in a stronger curvature of the coastline. It was expected that the coastline orients itself perpendicular towards the incident wave direction, which was not the case when default XBeach parameters were used. It is therefore very likely that sediment transport towards the exposed coastline is underestimated by XBeach in the previous model set-ups. In Appendix A, a sensitivity analysis can be found on the shoreline response using various sediment transport calibration factors. This analysis showed that the onshore sediment transport increased with increasing calibration factors (f_{Sk}, f_{As}). These findings were in line with the expected response according to Eq. 8.

Higher values for the calibration factors were therefore found to increase the model performance (qualitatively). Straightening of the coastline could now be observed instead of the increased curvature (see Figure 7). Based on *QC 1.4* and *QC 1.6*, values of 0.15 for both factors were found to be appropriate according to the expected morphological changes.

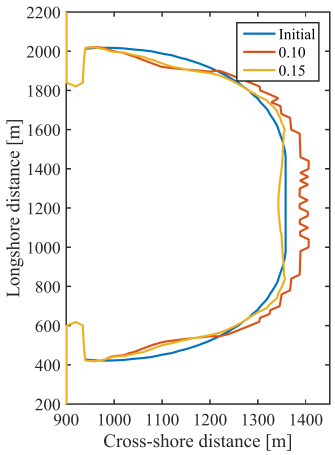

Figure 7: Shoreline response using different values for both of the sediment advection calibration factors. The final bathymetry contour line at -1 meter is given for values of 0.10 (default) and 0.15. For these simulations, the Van Thiel-Van Rijn sediment transport formulation was used.

Shoreline Rotation

High longshore flow velocities were found when performing stationary XBeach calculations for oblique waves without the bathymetry adjustments presented on Page 10. These flow velocities caused unrealistic erosion in front of the headlands and rapid bay filling, making the assessment of the qualitative checks troublesome. The solution was found in applying the same bathymetry correction as in the case of normal waves.

Hydrodynamics such as the expected inflow from the up-drift headland (*QC 2.1*) and the longshore current inside the pocket (*QC 2.2*) were represented with the stationary wave model. Sedimentation and erosion did occur as expected (*QC 2.3*). The morphological response of the pocket beach using the stationary mode did show shoreline rotation (*QC 2.4*), but this shoreline was quite irregular. A large erosion patch around the down-drift headland was furthermore modelled, which might impact the final model results.

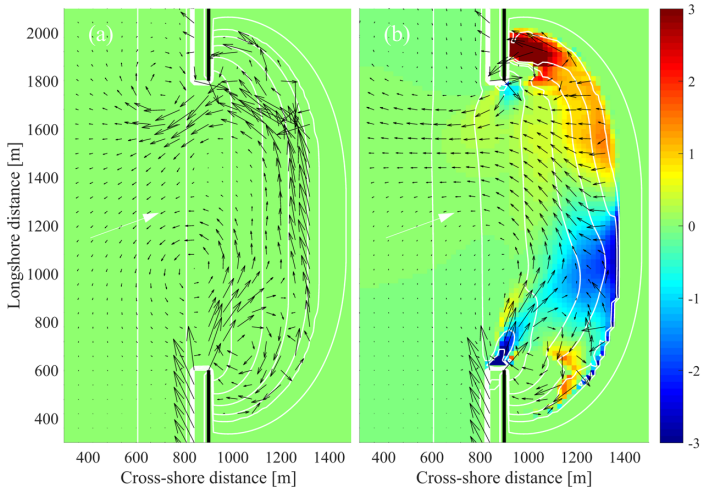

Figure 8: The initial conditions (a) and morphological response (b) of pocket beaches under 250 degree wave conditions using the stationary mode. Colours indicate sedimentation and erosion patterns. Wave current interactions are disabled, black vectors indicate the Eulerian velocity directions. Depth contour lines are given in white, ranging from -12 meters to +2 meters with intervals of 2 meters. The white arrow indicates the mean wave direction and its length corresponds to 1 m/s. The following wave climate was applied: H_s = 2 m, T_{m01} = 10 s, Dir = 250° and Dspr = 10.

Surfbeat and Non-Hydrostatic Modes

Calculations performed using the surfbeat mode within XBeach showed that higher sediment transport calibration factors were required compared to stationary calculations (see Figure 9). Under normal wave attack, the rip current was less visible than in the stationary mode. This can be attributed to the spatial varying wave height in the surfbeat mode, averaging the Eulerian velocity over time (30 hours) was used to capture the rip current but it was found to be rather difficult (*QC 1.2* and *QC 1.3*). The morphological response was modelled as expected, although the sediment advection calibration factors had to be increased to 0.30 (based on *QC 1.4* to *QC 1.6*). Under oblique wave attack, the hydrodynamics were well represented in the surfbeat mode. Inflow from the up-drift headland and outflow from the down-drift headland can be observed, which is in line with *QC 2.1* and *QC 2.2*. Compared to the study by Daly et al. (2011), the morphological response under oblique waves was similarly modelled. Sedimentation behind the down-drift headland can be observed whereas erosion dominates the area behind the up-drift headland (*QC 2.3* and *QC 2.4*). Under both wave conditions, a 'smoother' coastline was modelled using the surfbeat mode when compared to stationary runs. The up-drift erosion patch that was observed using the stationary wave model (see Figure 8b) is almost non-existent when using the surfbeat model (see Figure 9d).

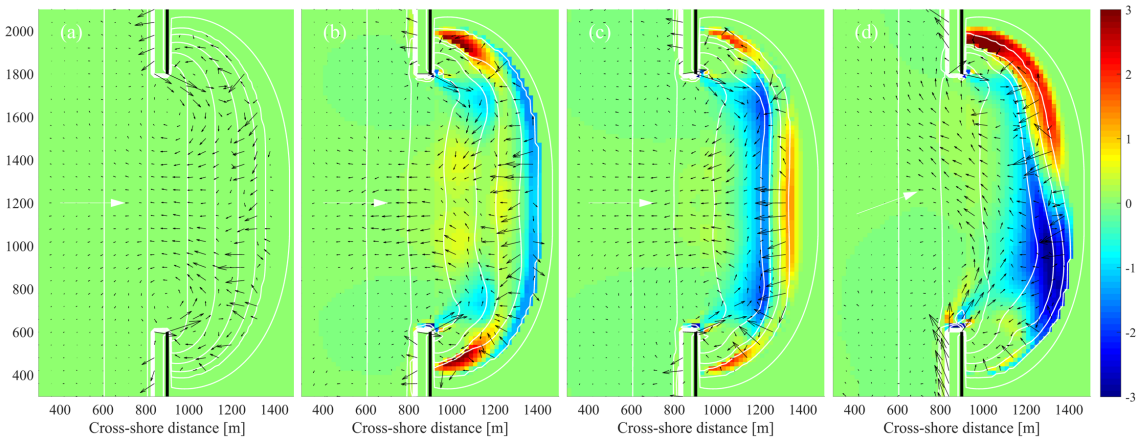

Figure 9: Morphological response of pocket beaches under 270° wave conditions (b, c) and 250° wave conditions (d). Sediment calibration factors of 0.15 (b) and 0.30 (c, d). Colours indicate sedimentation and erosion patterns. Wave current interactions are disabled, black vectors indicate the Eulerian velocity directions (averaged over 30 hours). Depth contour lines are given in white, ranging from -12 meters to +2 meters with intervals of 2 meters. The white arrow indicates the mean wave direction and its length corresponds to 1 m/s. The following wave climate was applied: H_s = 2 m, T_{m01} = 10 s, Dir = 250°/270° and Dspr = 10.

Non-hydrostatic simulations turned out to be very computationally demanding. Using a morphological acceleration factor of 10, computational times exceeded 80 hours on 14 cores. Simulations did succeed however with a much higher factor of 50, leading to acceptable (+14 hours) simulation times on multiple (14) cores (3101 MHz). The results showed that the expected diffraction around the headlands is modelled by the non-hydrostatic mode (see Figure 10a). Under both wave conditions (shore normal (b) and oblique wave attack (c)) it can be seen that a 'ring' of erosion does occur just below the still water line. Under shore normal wave forcing it can be seen that sediment is deposited behind both of the headlands, in compliance with *QC 1.6*. Under oblique wave attack, the sediment is mostly transported towards the down-drift headland, which is in line with *QC 2.3*. Erosion occurs mainly behind the up-drift headland and some sedimentation can be observed directly behind this structure (*QC 2.3*). In front of the headlands, the non-hydrostatic model does show some morphological activity. Wave-like sedimentation and erosion patterns can be observed with a 'wavelength' of approximately 60 meters.

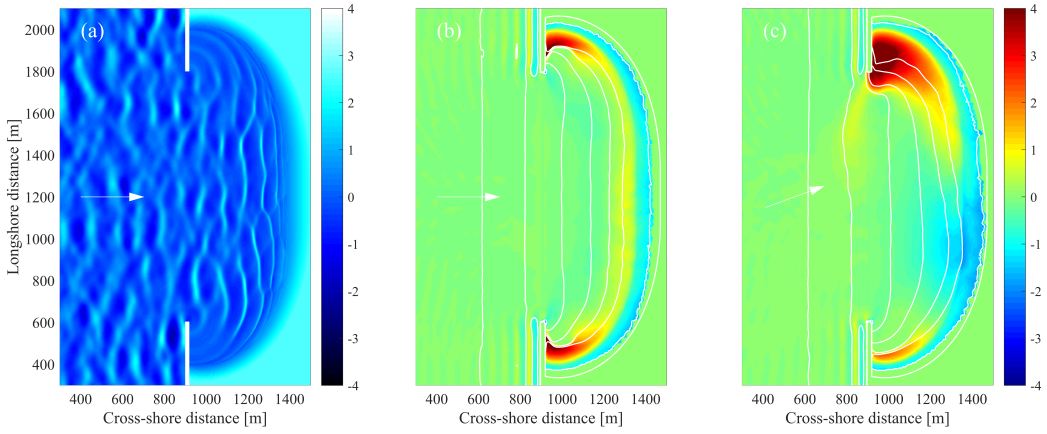

Figure 10: Water level (a) and sedimentation erosion results obtained from non-hydrostatic model calculations. The morphological response of the pocket is given for shore normal wave forcing (b) and under oblique wave attack (c).

Intermezzo 1: Expansion of the Classic Pocket Beach

In reality, the classic pocket beach (as used in the previous sections) is often found to be part of a more complex system. One of these more complex systems is created when pocket beaches are adjacent. These pocket beaches can either be separated by tombolos or by salients.

A clear distinction between these two systems is therefore challenging to formulate. Wave setup differences (causing additional circulation patterns) within the salient systems could lead to a completely different behaviour when compared to tombolo systems. It is of great interest whether it is sound to assess individual pockets when adjacent pockets are present. The hypothesis that is tested in this intermezzo is thus formulated as follows;

Tombolo and salient pocket beach systems respond differently to wave forcing than individual pocket beaches.

The schematic model setup presented in Part 1 of this study was used to verify this hypothesis. First, the morphological development of a single pocket beach under normal wave conditions (270°) was modelled with the surfbeat mode. Second, the resulting bathymetry was duplicated, creating two adjacent pocket beaches. Duplication was done in two ways; with a tombolo (L/D = 1.3) or a salient (L/D = 0.5) behind the offshore breakwater (after Bricio et al. (2008)). Third, the morphological development of these adjacent pocket beaches was modelled. A flow chart depicting the described steps can be found in Appendix B (see Figure 21).

When assessing the average modelled erosion per timestep, it can be seen that the morphological development has a positive feedback on the system (Figure 11). This can be concluded from the stabilisation in average modelled erosion. After duplicating the model, either forming a tombolo or a salient behind the breakwater, it can be seen that the models require some time to approach a new equilibrium[2]. It is clear that the model in which a salient was formed after duplication, a larger mismatch in averaged modelled erosion can be observed (see jump at t=360 in Figure 11). Corresponding sedimentation and erosion patterns can be found in Appendix B (see Figure 22).

It can therefore be concluded that the modelling of adjacent pocket beaches with a tombolo shows reasonable similarities to modelling of single pocket beaches. These adjacent pocket beaches can therefore be modelled individually with XBeach, reducing the amount of computation time required. If a salient is present between two adjacent pocket beaches, the system will behave in a different way, making it obligatory to model the entire pocket beach system. An individual assessment of pockets separated by salients will otherwise result in unreliable model predictions.

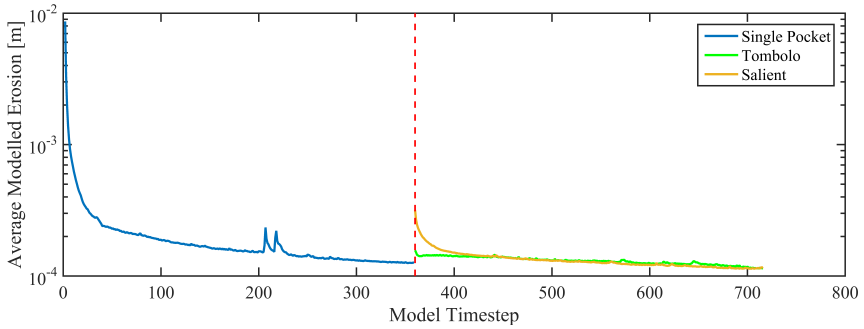

Figure 11: The average modelled erosion in the classic pocket beach case (t = 1:360) and the expansion towards a Tombolo or Salient system (t = 360:720).

[2]Reference is made to the '*Dynamic 1 Equilibrium Condition*' as defined in the paper by Zhou et al. (2016)

DISCUSSION

The morphological development of pocket beaches is highly dependent on the hydrodynamics within these systems. The results show that in order to predict the bed level, an correct representation of the flow patterns is essential. The initial model setup showed an agreement with the expected flow patterns inside the pocket. Outside the pocket, a net inflow around the headlands was non-existent however. In the paper by Daly et al. (2011), this was not observed, which indicates that the SWAN wave module within Delft3D is capable of calculating this local water level setup in front of hard structures without wave breaking. A net inflow around the headlands was therefore present in their study. After adding an artificial foreshore to the XBeach model, flow patterns were found that are in line with other pocket bay model results (Daly et al., 2011; Silva et al., 2010).

The results indicated that wave-current interaction within XBeach causes unrealistic wave patterns behind headlands. These patterns do not cause fatal instabilities, but the patterns suggest the introduction of numerical errors using WCI. This behaviour is in line with findings by Deltares, which does not advise using WCI due to the experimental status of this addition (Deltares, 2015). Although the importance of WCI has been shown in various studies on rip currents (Reniers et al., 2007; Yu and Slinn, 2003), this study found that inclusion of WCI was not found to outweigh the introduced errors in XBeach.

Under shore normal wave conditions and using the hydrostatic modes in XBeach, the morphological response was found to be less quick than presented in the study by Daly et al. (2011)[3]. This can be attributed to a combination of the hydrostatic mode and transport formula in XBeach. The hydrostatic mode in XBeach lacks a correct representation of diffraction, which reduces the sediment transport behind the headlands. As expected, the Soulsby-Van Rijn formulation did show more sedimentation in these areas compared to the Van Thiel-Van Rijn formulation. Non-hydrostatic modelling, with the Van Thiel-Van Rijn formulation, did produce these sedimentation patterns due to the fact that wave diffraction around the headlands is properly included in this mode. This implies that Van Thiel-Van Rijn underestimates the sediment transport without the presence of waves. The results have shown that the latter transport formula is preferred over Soulsby-Van Rijn however.

Under oblique wave attack, the modelled hydrodynamics and morphology showed reasonable similarities to the respective quality checks and the results presented in Daly et al. (2011). The expected inflow from the up-drift headland was represented, a longshore current was generated and sediment was transported as expected. The exception was the relatively low amount of sedimentation behind the up-drift headland, in contrast to Daly et al. (2011). The obtained hydrodynamic conditions under oblique wave attack were also in line with other pocket bay studies (Daly et al., 2011; Silva et al., 2010). The expected shoreline rotation (although somewhat unregular) was also modelled. A large patch of eroded material could however be observed around the up-drift headland using the stationary mode (see Figure 8b). This erosional feature is a response to the relatively high and constant flow velocity around the headland.

Comparing the stationary mode to the surfbeat mode when modelling coastline response under oblique wave attack, a 'smoother' coastline response was obtained using surfbeat. In addition, the erosion around the up-drift headland was greatly reduced. This can be attributed to the fact that the waves within the surfbeat mode have some variation around the mean (used in the stationary mode). Due to this variation around the mean, a larger sediment calibration factor was required to obtain the expected system response. One of the main reasons to prefer surfbeat modelling over stationary modelling is the inclusion of infragravity waves. These infragravity waves have been shown to be of importance in pocket beach modelling (Dehouck et al., 2009).

[3]Their paper does not specify which sediment transport formula within Delf3D was applied. By default the sediment transport formula of Van Rijn (1993) is used within Delft3D (Deltares, 2014). In this formulation the bed load transport is proportional to the current velocity to the power 2.4 (without waves), similar to the Soulsby-Van Rijn formulation in XBeach. The SWAN wave model used in their study does include an approximation of wave diffraction.

Non-hydrostatic modelling of shore-normal waves did succeed and showed the expected sedimentation behind the headlands due to the included diffraction. The initial cross-shore profile (determined using Dean (1991)) showed erosion around the upper shoreface creating a 'ring' around the mean sea level. This was also found in the hydrostatic modes but could be reduced by changing the sediment advection calibration parameters for those simulations. This was not possible in the non-hydrostatic simulations due to the independence of the discretization for the advection velocity (Eq. 8). Non-hydrostatic modelling of oblique waves showed a significant increase in transported sediment volumes. The unexpected morphological changes modelled using the non-hydrostatic mode can be explained by the transport formulas used. The sediment transport formulas implemented in XBeach have been properly validated for the hydrostatic modes, whereas the morphological performance of the non-hydrostatic modes (2D) is still unknown (Deltares, 2017).

CONCLUSION

The open source XBeach model can be used to assess pocket beach behaviour under (non)normal wave forcing. Under both normal and oblique wave attack, the surfbeat mode can be advised. Bed level adjustments to the schematized model had to be made in order to represent the hydrodynamic conditions around the entrance of the pocket.

Wave-current interaction, which is often seen as an important feature when modelling rip currents, was found to produce unreliable model results. A more pronounced rip current did occur, but this did not outweigh the errors that are introduced by WCI. Unexpected wave conditions were found behind the headlands, showing some resemblance to a numerical error in these sheltered areas. It is therefore suggested that WCI should be avoided when modelling pocket beaches using XBeach.

The sediment transport formulation of Van Thiel-Van Rijn showed that sedimentation behind the headlands was rather limited. This is due to the importance of wave presence within their formulation. The Soulsby-Van Rijn transport formulation did show more sedimentation behind these headlands, but showed large erosion in the pocket centre. It was therefore found that Van Thiel-Van Rijn (despite the low amounts of sedimentation behind the headlands) outperforms the Soulsby-Van Rijn formulation when applied to pocket beaches. Compared to previous numerical studies on pocket beach morphology, it was found that the morphological response is much quicker when using Delft3D. The source of the difference between the sedimentation rates behind the headland can thus be attributed to the difference in sediment transport formulations and implementation.

Straightening of the shoreline is heavily influenced by the choice of calibration factors f_{As} and f_{Sk}. It was found that the default values (0.10) for these parameters do not produce the expected shoreline straightening. An increased value (0.15) for both of these parameters is found to be sufficient in the stationary simulations. Simulations performed using the surfbeat mode showed that a further increase of these factors to 0.30 was required to produce the expected shoreline straightening.

The surfbeat mode within XBeach outperformed both the stationary and non-hydrostatic modes for the pocket beach schematizations. The stationary performed significantly worse than surfbeat under oblique wave attack and the non-hydrostatic produced a 'circle' of erosion resulted around the upper shoreface. The non-hydrostatic mode was found to be quite promising and was able to simulate the wave diffraction around the headlands. The sediment transport formulas implemented within XBeach still have to be improved for this mode however.

Expanding the classic pocket beach system proved the need for a complete model setup if interactions between two pockets are expected. It was shown that if a fully developed tombolo is formed between the pockets, the pocket beaches can be modelled individually without the introduction of major errors in the schematization. If a salient is present between the pockets, a complete schematization of the system should be made due to wave set-up differences behind the offshore breakwater. This study has shown that a significant difference in morphological response of the pocket beach can otherwise lead to invalid interpretations of the pocket beach system.

Further studies are necessary to determine the differences between XBeach and Delft3D when implementing the same sediment transport formulations in both models. On the subject of sediment transport formulas, additional research could prove whether these formulations hold for non-hydrostatic simulations or have to be improved upon. Fine tuning of the sediment adaptation time (used in the advection-diffusion scheme of XBeach) could result in more sedimentation behind the headlands. Studies into the possible mimicking of diffraction by increasing the directional spreading of hydrostatic models (especially surfbeat) could be of great value as well.

Part II
Tanjong Beach, Singapore - Case Study

Part 2 of this paper consists of a case study on the long term morphology of pocket beaches at the island of Sentosa, Singapore (see Figure 12). One of these pocket systems, Tanjong Beach, is selected for this case study. After creating a model setup, bathymetric measurements between 2000 and 2015 are used to assess the skill of the long term morphological computations. Preliminary XBeach model setups for Sentosa have been created by Witteveen+Bos (W+B) and will be used as a starting point of this part. The findings of Part 1 will be used to determine appropriate model settings for Tanjong Beach.

STUDY AREA

Sentosa is one of Singapore's offshore islands especially designed for recreational activities. With an area of approximately 5 km^2, this island sees close to 20 million visitors each year and an estimated 6 million of these visit the three main beaches on Sentosa: Siloso, Palawan and Tanjong (Sentosa Development Corporation, 2016). The total shoreline length of these beaches combined is about 2.4 km. Located in the Singapore Strait, the environmental conditions at Sentosa are relatively mild. The tidal range is around 3 m with only little variations between the seasons (maximum of 10 cm in MSL). Waves are governed by locally generated wind and ship waves (swell waves are not present) due to the natural sheltering properties of the Singapore Strait. Despite these mild conditions, a retreat of the coastline forces the local authorities to perform regular maintenance of these beaches.

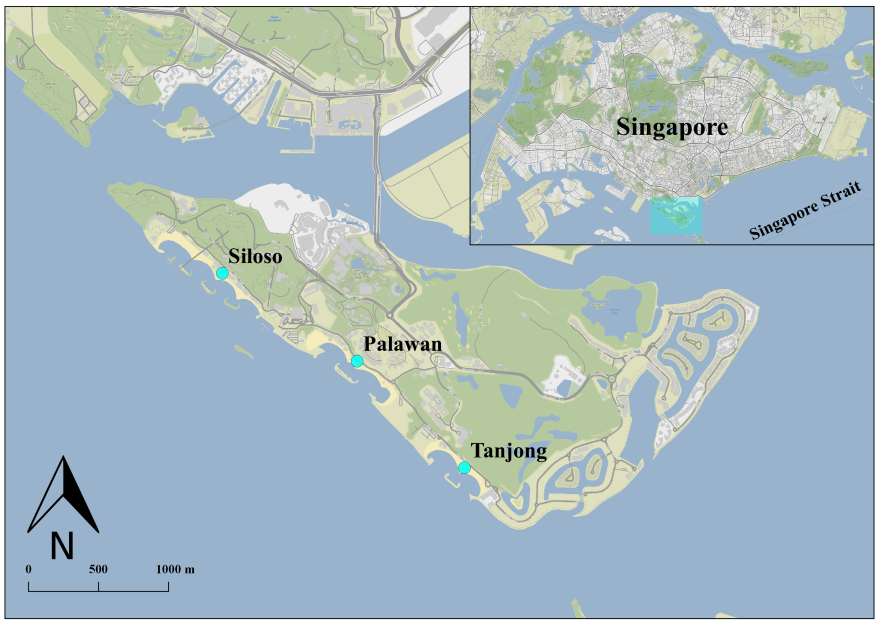

Figure 12: Overview of the Sentosa Island (blue rectangle) in Singapore. The three main beaches Siloso, Palawan and Tanjong are indicated on this map.

18/4/2000 06/04/2008 03/05/2016

Figure 13: Satellite imagery of Tanjong Beach showing the morphological development between the year 2000 and 2016. (Source: DigitalGlobe, 2016).

The satellite images[4] of Figure 13 show a clear development of a salient behind the emerged offshore breakwater. Noticeable sedimentation has also occurred behind the northwest headland. The provided bathymetric data is in line with the observations from satellite imagery and shows the formation of a salient at Tanjong Beach (see Figure 14). A plot of the sedimentation and erosion, which is defined as the 2015 bathymetry subtracted by the 2000 bathymetry, gives a better understanding of the morphological changes (see Figure 15). This figure clearly depicts sedimentation behind the offshore breakwater, erosion at the exposed shoreline (centre of the pockets) and sedimentation behind the northwest headland. Bathymetric contour lines (at z = 0) show a counter clockwise rotation of the shoreline between 2000 and 2015 (see Figure 15). Erosion can be observed around the offshore breakwater. The breakwater (which was constructed on top of an existing coral reef) might have settled over time, leading to the depicted 'erosion'.

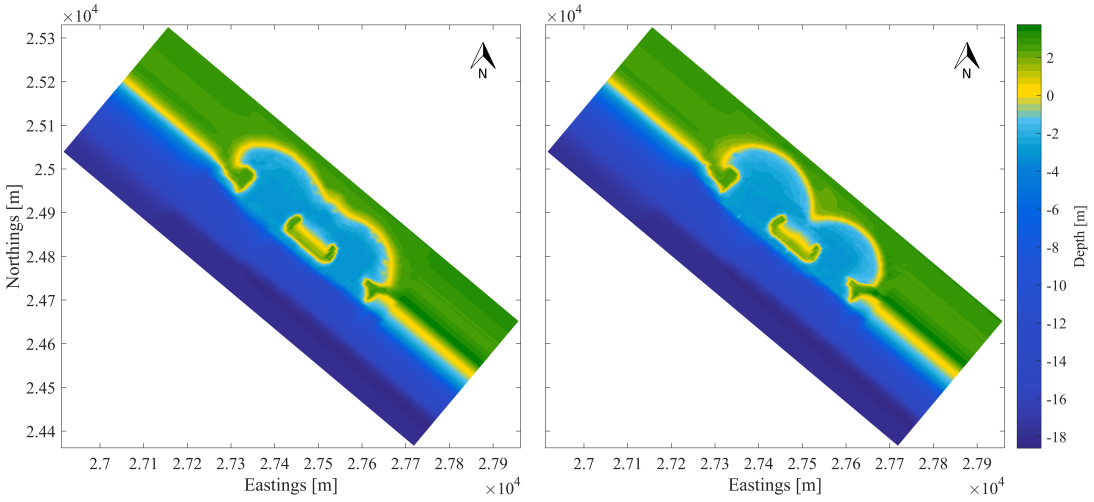

Figure 14: Bathymetric data of Tanjong Beach showing the bed level in 2000 (left) and 2015 (right).

[4]Note that the differences in water levels (due to tides) limits the usability of these images. Methods have been developed to improve the understanding of shoreline behaviour from satellite images (e.g. Garcia-Rubio et al. (2012)), but were found to be outside of the scope of this study.

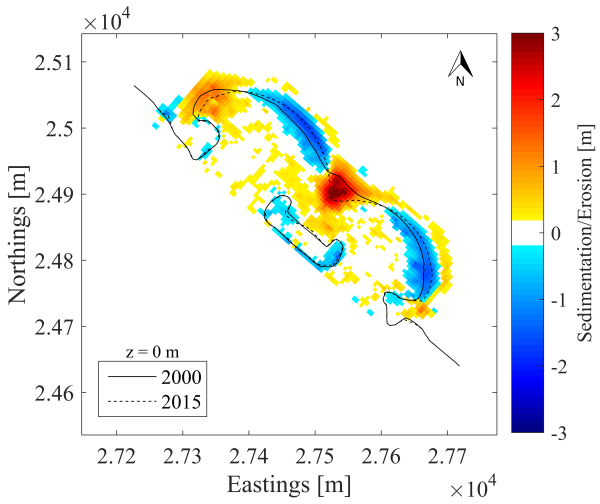

Figure 15: Cumulative sedimentation and erosion of Tanjong Beach between the years 2000 and 2015. The black solid and dashed lines represent the shorelines at the year 2000 and 2015 respectively.

As stated previously, local authorities have performed maintenance to the beaches of Sentosa (see Figure 16). Actions had to be taken due to the retreat of the coastline in the centre of each pocket. Using relatively simple equipment, sediment was transferred from the tombolo to the exposed shorelines. It is assumed that these sediments stay within the system and have no major impact on the equilibrium coastline orientation of Tanjong Beach. Additional sediment was introduced into the system from a stockpile located at Sentosa. It is therefore expected that the amount of sedimentation behind the northwest headland will be under-predicted by the model.

Figure 16: The performed maintenance by the Sentosa Development Corporation. Sediment from the tombolo has been distributed over the (mostly) exposed coastline and sediment has been added from the stockpiles. (Sentosa Development Corporation, 2016)

The environmental conditions (water levels and waves) have been determined as part of an ongoing project concerning the beaches of Sentosa. This data has been provided by Witteveen+Bos (W+B). Water levels have been derived from a calibrated Delft3D model for the Singapore Strait (see Figure 17). Unfortunately, no wave measurements are available at Tanjong Beach. Wave data has therefore been derived by W+B, using alternative sources. During their assessment of the Sentosa beaches, locally generated (ship) waves have been found to be dominant. A combined wave climate has been deduced by W+B from ship sailing speeds and the governing wind conditions southwest of Sentosa. These wave conditions have been translated using SWAN to the boundary conditions for the XBeach model (see Figure 17). Note that in the study by W+B a schematization of the governing waves around Sentosa was performed, reducing the amount of computational effort required for the models. It was found that a year of wave data can be reduced to 75 days of wave data that has the same impact on the beaches at Sentosa (wind and ship).

After a site visit, expert judgement estimated the sediment grain size to vary between 140 μm and 300 μm. A D_{50} of 250 μm is found to be reasonable for Tanjong Beach.

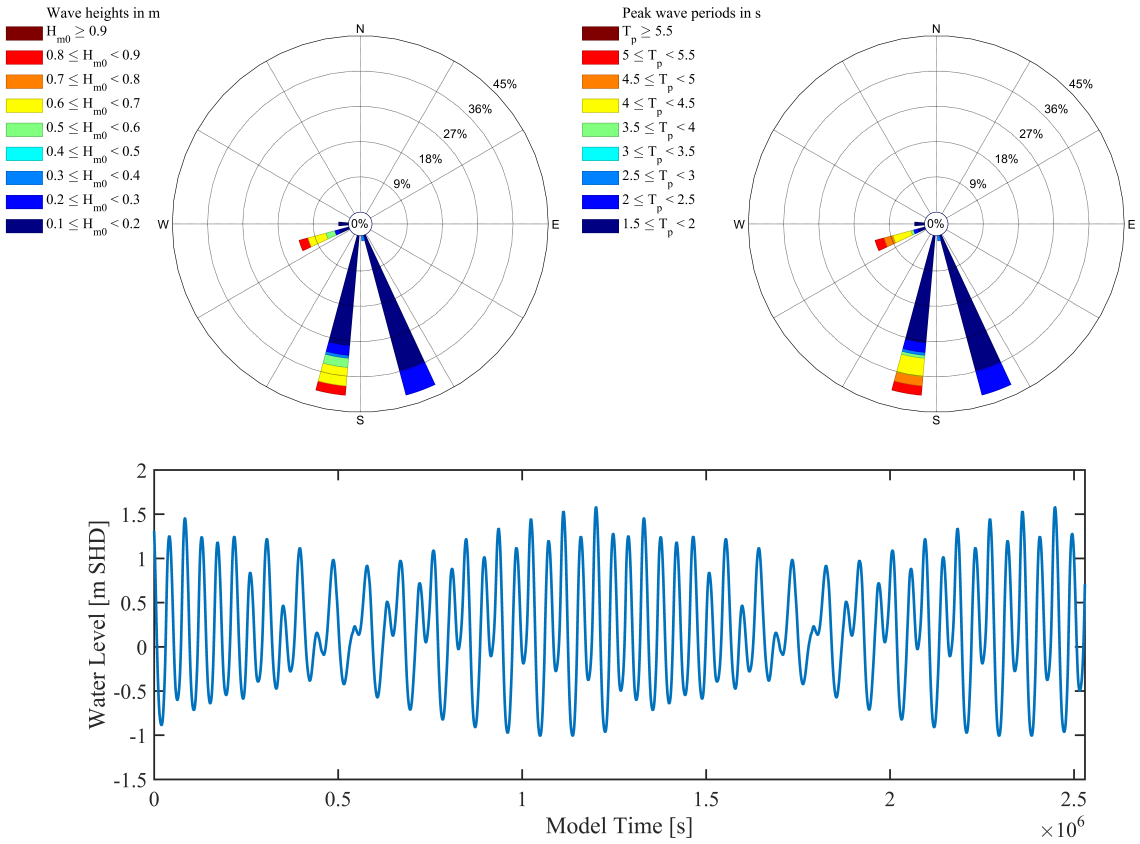

Figure 17: Wave conditions at Tanjong Beach, H_{m0} (top left) and T_p (top right). Tidal conditions (bottom) with respect to Singapore Height Datum at Tanjong Beach, derived from a Delft3D model of the Singapore Strait.

MODEL SETUP

The XBeach settings that were found to be valid for pocket beaches (see Part 1) have also been applied to this case study. Due to the fact that Tanjong Beach does show formation of a salient, a complete model of the system had to be made (see Intermezzo 1 and Appendix B). It was furthermore found that the surfbeat mode outperformed the stationary wave mode within XBeach. The surfbeat mode has therefore been used for this case study, modelling Tanjong Beach under (mostly) oblique wave attack. A brief overview of model parameters has been given in Table 2, default XBeach settings were used if not specified differently.

Mode		**Surfbeat**
Gridsize [m]	Max	10
	Min	3
Wave Directional Grid	θ_{max}	140
	θ_{min}	-40
Morfac		50
Sediment Calibration Factors	f_{As}	0.30
	f_{Sk}	0.30
Wave Breaking	Formulation	Roelvink1
	Gamma	0.55

Table 2: Overview of the XBeach parameters that are used in this case study for surfbeat and non-hydrostatic modes.

The numerical grid that has been derived for this XBeach model can be found in Figure 18. This grid has been created using the Delft3D grid generation module; RGFGRID. This grid complies with smoothness and orthogonality criteria in x and y directions. Bathymetric samples have been processed using the Delft3D data interpolation module; QUICKIN. The obtained Delft3D grid was then transformed to an XBeach grid using `XB_grid_delft3d.m` from the Open Earth Tools.

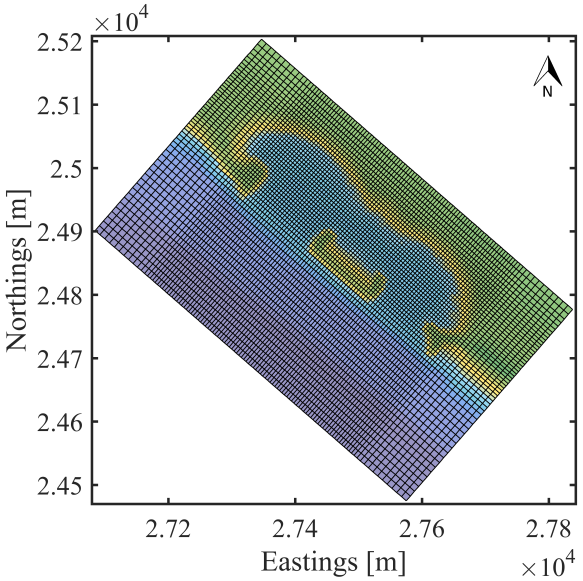

Figure 18: Tanjong Beach XBeach grid on top of the initial bathymetry from the year 2000.

SKILL ASSESSMENT

The Mean-Squared Error Skill Score (MSESS) was computed to indicate the performance of the model. This method of judging the accuracy of morphodynamic models is often referred to as the Brier Skill Score (BSS) and is popular amongst coastal scientists. Bosboom et al. (2014) showed that the MSESS can result in an overestimation of the model skill and has to be validated by expert judgement.

This skill score was implemented according to the description given in Bosboom et al. (2014);

$$MSESS_{ini} = 1 - \frac{MSE}{MSE_r} \tag{17}$$

Where MSE represents the Mean-Squared Error of the model and MSE_r represents the Mean-Squared Error of the reference case. This reference case often describes zero morphological development. The model therefore has to outperform a prediction of zero changes in the bathymetry. This reference case was also used in this study. In order to calculate the MSE between the modelled and observed bathymetries the following equation was used (obtained from Bosboom et al. (2014));

$$MSE = 1 - \langle (p-o)^2 \rangle = \frac{1}{n} * \sum_{i}^{n} w_i (p_i - o_i)^2 \tag{18}$$

Where the angled brackets indicate a spatial (weighted) averaging, which is represented by w_i in the final form. The predicted and observed fields are represented by p_i and o_i respectively. No readily available toolbox could be used to compute the skill scores for a non-uniform 2D grid. These formulas have therefore been implemented in a `MATLAB` script (see Appendix 3).

	$MSESS_{ini}$
Excellent	1.0 - 0.5
Good	0.5 - 0.2
Reasonable/fair	0.2 - 0.1
Poor	0.1 - 0.0
Bad	< 0.0

Table 3: $MSESS_{ini}$ classification as presented in Sutherland et al. (2004).

RESULTS

The XBeach model showed promising results when compared to the bathymetric measurements between 2000 and 2015 for Tanjong Beach (see Figure 19). The shoreline response that was predicted by the model was in agreement with the measured bathymetry of 2015. Behind the offshore breakwater the development of a salient was modelled and the coastline retreat at the exposed parts of the beach was predicted using the model. Sedimentation behind the northern headland was furthermore modelled using XBeach, whereas erosion dominated the morphological response behind the southern headland. The sedimentation and erosion patterns that were modelled resulted in a counter clockwise rotation and retreat of the shoreline, which corresponds to the measured bathymetry.

The model results show that the amount of erosion around the exposed shoreline is not equal in both parts of Tanjong Beach. The intensity of erosion at the northern coastline is higher (indicated by the dark blue colours), whereas the erosion at the southern side seems to be more spread out. At the lee side of the offshore breakwater no coastline changes have been modelled using the XBeach model.

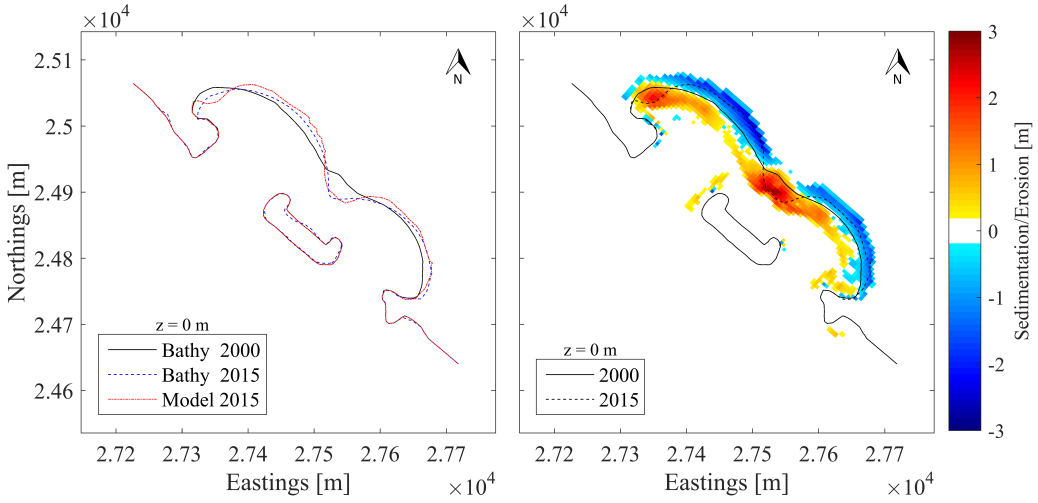

Figure 19: The shoreline response of the XBeach model compared to the bathymetric measurements done in 2000 and 2015 (left). On the right, the modelled cumulative sedimentation and erosion of Tanjong Beach between the years 2000 and 2015 is given.

The observed similarities between the model results and the measurements were in line with the skill score used in this study. The Mean-Squared Error Skill Score was found to be within the 'Good' region according to the classification scale by Sutherland et al. (2004). The skill score achieved by the model was equal to 0.31, which was in line with the visual assessment of coastline response and sedimentation and erosion patterns.

DISCUSSION

Sedimentation behind the offshore emerged breakwater is correctly represented by the XBeach model. Due to the limited wave action in this sheltered area, sediment collects and forms a salient over time. It can be seen from the results that the measured salient has a different profile compared to the computed salient. The measured coastline is more V-shaped than the modelled coastline, which is rather smooth. This finding is in line with the results obtained in Part 1. When expanding the classic pocket beach model into a more complex salient system, clear smoothing of the salient could be observed. This can be attributed to the fact that wave diffraction is not correctly implemented in the surfbeat mode. Due to the lack of this phenomena, sediment is not transported towards the middle behind the breakwater. Sediment is directly deposited behind the breakwater, were waves are underestimated by the surfbeat mode.

Sedimentation behind the northern headland was found to be slightly underestimated by the XBeach model. This can be explained from the applied maintenance at Tanjong Beach. During the maintenance operations performed, additional sediment was added to the system on the northern part of Tanjong Beach (see Figure 16). This human intervention has not been implemented in the XBeach model of this study.

The measured erosion in close vicinity to the offshore breakwater (see Figure 15) is not represented in the XBeach results (see Figure 19). This can be explained by the fact that settling of the breakwater has most likely occurred, leading to the measured 'erosion'. This behaviour has not been included in the XBeach model, but one could choose to remove this area from the bathymetric measurements. This would lead to an even higher Mean-Squared Error Skill Score, resulting in a higher model performance.

Calibration of the model has not been performed for this specific case. The parameter settings that were found to work for the schematizations of Part 1 have been applied, with the exception of the grain size. Despite this, a 'Good' model performance is obtained, which indicates that the set of parameters could be used for other cases as well. A calibration of the model could result in an even better model performance, but was found to be outside the scope of this study.

CONCLUSION

Despite the fact that limited data was available for Tanjong Beach, the XBeach model that has been set-up for this case study was found to produce similar morphological developments as have been measured between 2000 and 2015. This case study has shown that modelling (complex) pocket beach systems using XBeach is not only possible for schematized cases, but also for coastal engineering purposes. The obtained model, which has not been calibrated, showed a 'good' prediction of the morphological developments at Tanjong Beach. Due to the fact that this process-based approach allows for 'what-if' games, engineering solutions can now be designed and validated using this model. For example, to reduce the shoreline retreat at the site beach nourishment strategies can be assessed and wave reduction measurements can be tested.

Differences between the model calculations and the bathymetric measurements can be related to various sources (human interaction or local breakwater settlements). The formation of the salient however, is still very interesting. Both in Part 1 and Part 2, XBeach produces a rather smooth looking salient whereas measurements indicate the salient to be more V-shaped. Non-hydrostatic modelling could be applied to obtain the measured salient shape, due to the inclusion of wave diffraction. This mode is however not yet suitable for the sediment transport formulations implemented in XBeach.

Calibration of the model could improve the performance. Additional measurements, especially the wave conditions inside the pocket could be of great value. Despite these shortcomings the model was found to perform adequate and the model settings can be used for the other beaches of Sentosa.

Part III
Appendices and References

Appendix A. Sediment Transport Sensitivity Analsysis

The Van Thiel-Van Rijn the Soulsby-Van Rijn transport formula as can be seen in the results of Part 1. In this appendix the effect of changing the sediment advection calibration parameters can be found. These parameters (f_{As},f_{Sk}) influence the sediment advection velocity (see Eq. 8) which in turn impacts the advection-diffusion scheme implemented in XBeach (see Eq. 7). It was chosen to vary both of these parameters simultaneously in order to observe the changes in onshore sediment transport. Changing these parameters individually would not increase the performance of the model due to the schematized nature of this set-up. This sensitivity analysis mainly focusses on how to influence the onshore sediment transport in the centre of the pocket beach.

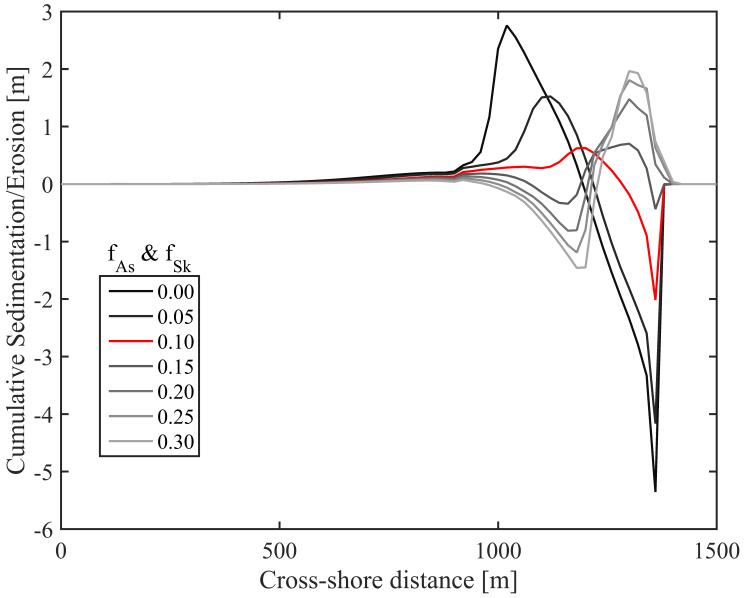

Figure 20: Cumulative sedimentation and erosion along the cross-shore distance at y = 1200 m (center of the pocket). Van Thiel-Van Rijn sediment transport formulation with varying calibration factors (Default 0.10).

From this figure it can be seen that the onshore sediment transport does increase with an increase in the calibration factors. This can be deduced from the fact that the cumulative sedimentation onshore increases with an increase of these factors. At the same time, 'offshore' (between 800 and 1200 m) sedimentation decreases and changes to erosion when applying larger than default values for the calibration factors. These findings are in line with the study by Bugajny et al. (2013), in which higher values for f_{ua} (abbreviation for both parameters) were found to better represent the onshore sediment transport in their system.

Appendix B. Expansion of the Classic Pocket Beach

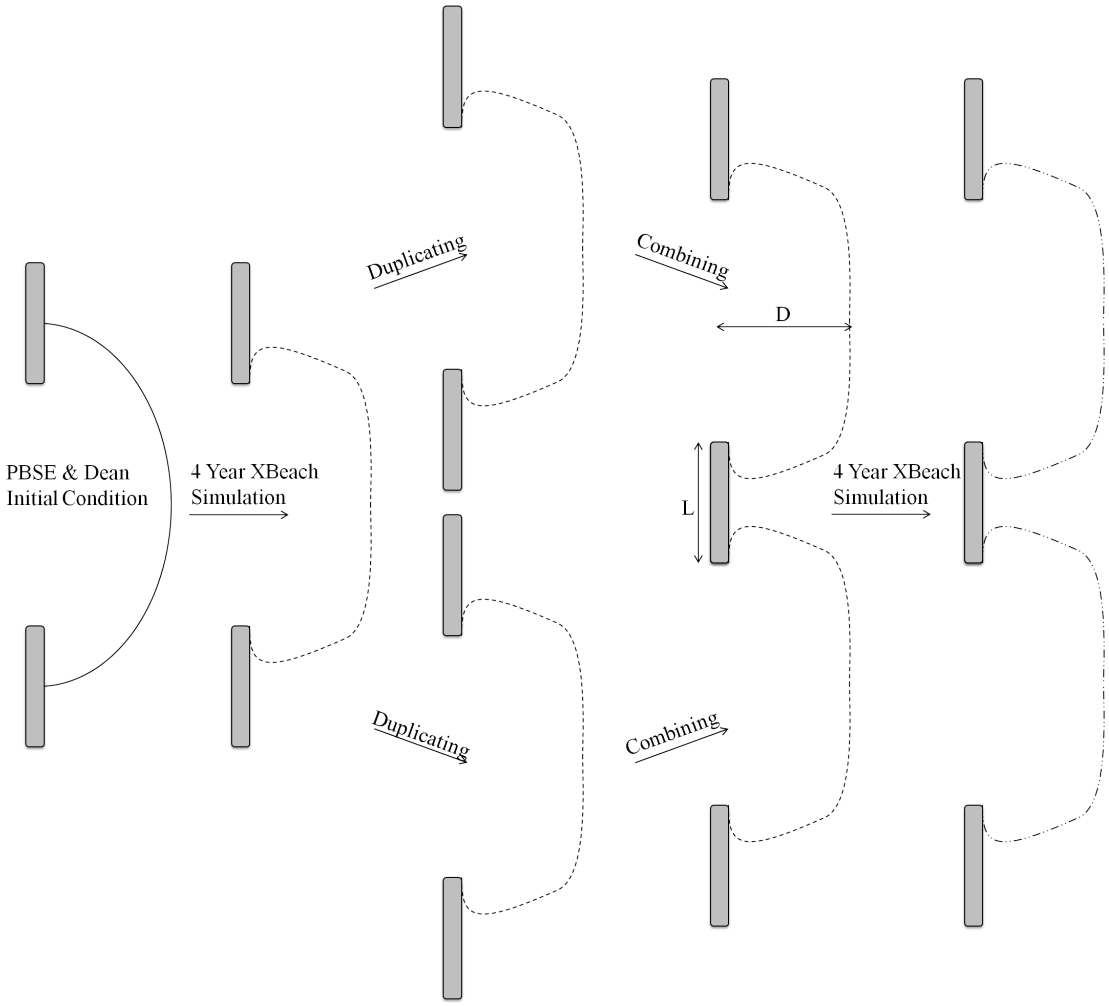

Figure 21: Flow chart representation of the method applied for pocket beach expansion. The solid line represents the initial condition, the dashed line represents the obtained shoreline after a four year simulation of the classical pocket beach and the dotted dash line is the result of a four year simulation of the combined system.

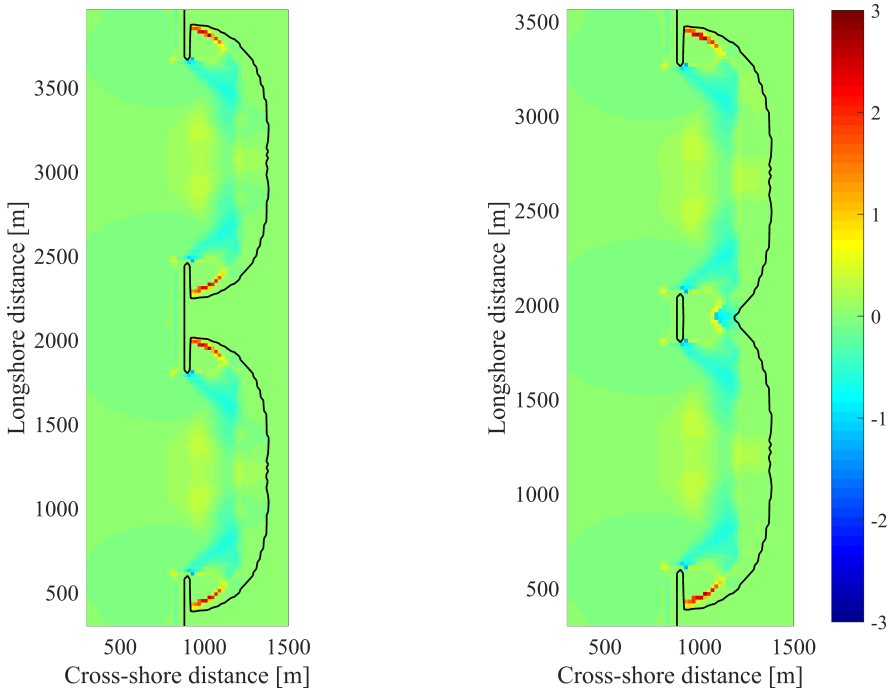

Figure 22: Sedimentation and erosion figures of the salient and tombolo systems. Colours indicate sedimentation and erosion patterns. The following wave climate was applied: H_s = 2 m, T_{m01} = 10 s, Dir = 270 and Dspr = 20.

From this figure it can be seen that the major difference in average modelled erosion (see Figure 11) for the salient system is present behind the breakwater. The tombolo system shows sedimentation behind the breakwater, whereas the salient is partly eroded. This can be attributed to the lack of a correct representation of diffraction around the headland. The salient will tend to be 'smeared' over a larger area. This causes the salient to look diffusive instead of V-shaped.

Appendix C. Mean-Squared Error Skill Score in MATLAB

```
clear all;
close all;

%% Load Measured Bathymetries
cd 'PathToFiles';
zb2000 = load('bed2000.dep');zb2015 = load('bed2015.dep')

%% Load Surfbeat Model Run
cd 'PathToFiles'
nc_file = 'xboutput.nc';
zb_xbout = xb_read_output(nc_file,...                    % read output
        'vars', {'zb'});

% Peel the XB structure
zb_xbout_peel  = xs_peel(zb_xbout);
zb_xbout_dims    = xs_peel(zb_xbout_peel.DIMS);
x           = zb_xbout_dims.x;
y           = zb_xbout_dims.y;
t           = zb_xbout_dims.t;
timestep = xxx;
zb_xbout      = squeeze(zb_xbout_peel.zb(timestep,:,:));

%% MSESS / Brier Skill Score
sizey = size(y);            %Obtain grid size
length_x = sizey(1);        %Obtain length in x dir
length_y = sizey(2);        %Obtain length in y dir
Surface = zeros(sizey);     %Create empty matrix for surface

%Fill Surface Matrix
for j = 1:(length_y-1);
    for i = 1:(length_x-1);
        dist1 = sqrt((x(i,j+1)-x(i,j))^2+(y(i,j+1)-y(i,j))^2);
        dist2 = sqrt((x(i+1,j)-x(i,j))^2+(y(i+1,j)-y(i,j))^2);
        Surface(i,j) = dist1*dist2;
    end
end

%Compute Weigthed Matrix
WeigthedMatrix = Surface/sum(sum(Surface))

%Compute MSE between Prediction Model (zb_xbout) and Observation
MSE = 1/(length_x*length_y).*sum(sum(WeigthedMatrix.*(zb_xbout-zb2015)
    .^2))
%Compute MSE between Baseline (initial condition) and Observation
MSE_r = 1/(length_x*length_y).*sum(sum(WeigthedMatrix.*(zb2015-zb2000)
    .^2))

MSESS_ini = 1-MSE/MSE_r
```

Appendix D. Default Parameters in XBeach

The presented values and settings in this Appendix have been obtained from Roelvink et al. (2015).

Model time parameters
CFL = .7000

Physical constants
rho = 1025.0000
g = 9.8100
depthscale = 1.0000

Wave boundary condition parameters
taper = 100.0000
nmax = .8000
random = 1
fcutoff = 0.0000
nspectrumloc = 1
nspr = 0
trepfac = .0100
sprdthr = .0800
Tm01switch = 0
wbcversion = 3

Flow boundary condition parameters
tidetype = velocity
front = abs2d
left = neumann
right = neumann
back = abs2d
ARC = 1
order = 2.0000
carspan = 0
freewave = 0
epsi = -1.0000

Wind parameters
windth = 270.0000
rhoa = 1.2500
Cd = .0020
windfile = None specified
windv = 0.0000

Wave numerics parameters
scheme = upwind 2
snells = 0

Wave breaking parameters
alpha = 1.0000
n = 10.0000
gammax = 2.0000
delta = 0.0000
fw = 0.0000
fwcutoff = 1000.0000
breakerdelay = 1

Roller parameters
roller = 1
rfb = 0

Wave-current interaction parameters
wci = 0
hwci = .1000
cats = 4.0000

Flow parameters
bedfriction = chezy
bedfriccoef = 55.0000
nuh = .1000
nuhfac = 1.0000
smag = 1

Coriolis force parameters
wearth = .0417
lat = 0.0000

Bed composition parameters
ngd = 1
nd = 3
por = .4000
ucrcal = 1.0000
rhos = 2650.0000
dzg = .1000
sedcal = 1.0000

Flow numerics parameters
eps = .0050
umin = 0.0000
hmin = .2000

Sediment transport parameters
sws = 1
lws = 1
BRfac = 1.0000
facsl = 1.6000
z0 = .0060
smax = -1.0000
tsfac = .1000
turbadv = none
turb = bore averaged
Tbfac = 1.0000
Tsmin = .5000
lwt = 0
betad = 1.0000
sus = 1
bed = 1
bulk = 0
facDc = 1.0000
fallvelred = 0
dilatancy = 0
reposeangle = 30.0000
bdslpeffmag = roelvink total
bdslpeffini = none
bdslpeffdir = none

Morphology parameters
morfacopt = 1
wetslp = .3000
hswitch = .1000
dzmax = .0500
struct = 1
ne layer = nonero.txt

Sedtrans numerics parameters
thetanum = 1.0000
sourcesink = 0
cmax = .1000

Bed update numerics parameters
nd var = 2
split = 1.0100
merge = .0100
frac dz = .7000

References

Aubrey, D. (1979). Seasonal patterns of onshore/offshore sediment movement. *Journal of Geophysical Research*, 84(C10):6347.

Baldock, T., Holmes, P., Bunker, S., and Van Weert, P. (1998). Cross-shore hydrodynamics within an unsaturated surf zone. *Coastal Engineering*, 34(May):173–196.

Bosboom, J., Reniers, A. J. H. M., and Luijendijk, A. P. (2014). On the perception of morphodynamic model skill. *Coastal Engineering*, 94(August).

Bricio, L., Negro, V., and Diez, J. J. (2008). Geometric detached breakwater indicators on the spanish northeast coastline. *Journal of Coastal research*, pages 1289–1303.

Bugajny, N., Furmańczyk, K., Dudzińska-Nowak, J., and Paplińska-Swerpel, B. (2013). Modelling morphological changes of beach and dune induced by storm on the southern baltic coast using xbeach (case study: Dziwnow spit). *Journal of Coastal Research*, 65(sp1):672–677.

Castelle, B. and Coco, G. (2013). Surf zone flushing on embayed beaches. *Geophysical Research Letters*, 40(10):2206–2210.

Dail, H. J., Merrifield, M. A., and Bevis, M. (2000). Steep beach morphology changes due to energetic wave forcing. *Marine Geology*, 162(2-4):443–458.

Daly, C. J., Bryan, K. R., Roelvink, J. A., Klein, A. H. F., Hebbeln, D., and Winter, C. (2011). Morphodynamics of Embayed Beaches: The Effect of Wave Conditions. *Journal of Coastal Research SI*, 64(64):1003–1007.

De Vet, P. (2014). Modelling sediment transport and morphology during overwash and breaching events. page 187.

Dean, R. G. (1991). Equilibrium Beach Profiles : Characteristics and Applications. *Journal of Coastal Research*, 7(1):53–84.

Dehouck, A., Dupuis, H., and Sénéchal, N. (2009). Pocket beach hydrodynamics: The example of four macrotidal beaches, brittany, france. *Marine geology*, 266(1):1–17.

Deltares (2014). Delft3d-flow user manual: Simulation of multi-dimensional hydrodynamic flows and transport phenomena, including sediments. Technical report, Hydro-Morphodynamics.

Deltares (2015). Xbeach 1d - probabilistic model: Adis, settings, model uncertainty and graphical user interface. page 65.

Deltares (2017). Xbeach skillbed report, revision 5123. status update trunk default revision: 5123, Deltares, Rotterdamseweg 185 p.o. box 177 2600 MH Delft The Netherlands.

Galappatti, G. and Vreugdenhil, C. B. (1985). A depth-integrated model for suspended sediment transport. *Journal of Hydraulic Research*, 23(4):359–377.

Garcia-Rubio, G., Huntley, D., and Russsell, P. (2012). Assessing shoreline change using satellite-derived shorelines in progreso, yucatán, méxico. *Coastal Engineering Proceedings*, 1(33):79.

Halligan, G. H. (1906). Sand movement on the new south wales coast. In *Proceedings of the Linnean Society of New South Wales*, volume 31, pages 619–640.

Harley, M. D., Turner, I. L., and Short, A. D. (2015). New insights into embayed beach rotation: The importance of wave exposure and cross-shore processes. *Journal of Geophysical Research F: Earth Surface*, 120(8):1470–1484.

Harley, M. D., Turner, I. L., Short, A. D., and Ranasinghe, R. (2011). A reevaluation of coastal embayment

rotation: The dominance of cross-shore versus alongshore sediment transport processes, Collaroy-Narrabeen Beach, southeast Australia. *Journal of Geophysical Research: Earth Surface*, 116(4):1–16.

Hsu, J. R. C. and Evans, C. (1989). Parabolic Bay Shapes and Applications. *Proceedings of the Institution of Civil Engineers*, 87(4):557–570.

Hsu, J. R.-C., Yu, M.-J., Lee, F.-C., and Benedet, L. (2010). Static bay beach concept for scientists and engineers: a review. *Coastal Engineering*, 57(2):76–91.

Lewis, W. V. (1938). The evolution of shoreline curves. *Proceedings of the Geologists' Association*, 49(2):107–127.

Ratliff, K. M. and Murray, A. B. (2014). Modes and emergent time scales of embayed beach dynamics. *Geophysical Research Letters*, 41(20):7270–7275.

Reniers, A. J. H. M., Macmahan, J. H., Thornton, E., and Stanton, T. P. (2007). Modeling of very low frequency motions during. *Journal of Geophysical Research*, (July).

Roelvink, D., Reniers, A., van Dongeren, A., van Thiel de Vries, J., McCall, R., and Lescinski, J. (2009). Modelling storm impacts on beaches, dunes and barrier islands. *Coastal Engineering*, 56(11-12):1133–1152.

Roelvink, J. A., van Dongeren, A., McCall, R. T., and Rooijen, A. (2015). Xbeach technical reference : Kingsday release xbeach technical reference : Model description and reference guide to functionalities. (April).

Sentosa Development Corporation (2016). Sentosa development corporation - explore sentosa.

Short, A. D. and Masselink, G. (1999). *Embayed and structurally controlled beaches*. Handbook of beach and shoreface morphodynamics. John Wiley & Sons.

Silva, R., Baquerizo, A., Losada, M. Á., and Mendoza, E. (2010). Hydrodynamics of a headland-bay beach-Nearshore current circulation. *Coastal Engineering*, 57(2):160–175.

Silvester, R. (1960). Stabilization of sedimentary coastlines. *Nature*, 188(4749):467–469.

Smit, P., Stelling, G., Roelvink, D., van Thiel de Vries, J., McCall, R., van Dongeren, A., Zwinkels, C., and Jacobs, R. (2010). Xbeach: Non-hydrostatic model. *Report, Delft University of Technology and Deltares, Delft, The Netherlands*.

Sutherland, J., Peet, A., and Soulsby, R. (2004). Evaluating the performance of morphological models. *Coastal engineering*, 51(8):917–939.

Turki, I., Medina, R., Gonzalez, M., and Coco, G. (2013). Natural variability of shoreline position: Observations at three pocket beaches. *Marine Geology*, 338:76–89.

van Thiel de Vries, J. (2009). *Beach and dune erosion during storm surges*, volume 6.

Yu, J. and Slinn, D. N. (2003). Effects of wave-current interaction on rip currents. *Journal of Geophysical Research*, 108:1–19.

Zhou, Z., Coco, G., Townend, I., Olabarrieta, M., van der Wegen, M., Gong, Z., D'Alpaos, A., Gao, S., Jaffe, B. E., Gelfenbaum, G., et al. (2016). Is "morphodynamic equilibrium" an oxymoron? *Earth-Science Reviews*.